HHS Public Access

Author manuscript

Nat Commun. Author manuscript; available in PMC 2016 April 20.

Published in final edited form as:

Nat Commun. ; 6: 8608. doi:10.1038/ncomms9608.

Follicular Regulatory T Cells Impair Follicular T Helper Cells in HIV and SIV Infection

Brodie Miles[1], **Shannon M. Miller**[1], **Joy M. Folkvord**[1], **Abigail Kimball**[1], **Mastooreh Chamanian**[1], **Amie L. Meditz**[1,2], **Tessa Arends**[1], **Martin D. McCarter**[3], **David N. Levy**[4], **Eva G. Rakasz**[5], **Pamela J. Skinner**[6], and **Elizabeth Connick**[1]

[1]Division of Infectious Diseases, School of Medicine, Anschutz Medical Campus, University of Colorado Denver, 80045

[3]Department of Surgery, School of Medicine, Anschutz Medical Campus, University of Colorado Denver, 80045

[4]Department of Basic Science, New York University College of Dentistry, 10010

[5]Wisconsin National Primate Research Center, University of Wisconsin-Madison, 53715

[6]Department of Veterinary and Biomedical Sciences, University of Minnesota, 55108

Abstract

Human and simian immunodeficiency viruses (HIV and SIV) exploit follicular lymphoid regions by establishing high levels of viral replication and dysregulating humoral immunity. Follicular regulatory T cells (T_{FR}) are a recently characterized subset of lymphocytes that influence the germinal center response through interactions with follicular helper T cells (T_{FH}). Here, utilizing both human and rhesus macaque models, we show the impact of HIV and SIV infection on T_{FR} number and function. We find that T_{FR} proportionately and numerically expand during infection through mechanisms involving viral entry and replication, TGFβ signaling, low apoptosis rates, and the presence of regulatory dendritic cells. Further, T_{FR} exhibit elevated regulatory phenotypes and impair T_{FH} functions during HIV infection. Thus, T_{FR} contribute to inefficient germinal center responses and inhibit HIV and SIV clearance.

HIV rapidly establishes a productive viral infection in secondary lymphoid tissues, which is maintained during chronic stages of disease [1,2]. During chronic HIV infection, viral replication is highly concentrated within B cell follicles in follicular T helper cells (T_{FH}) [3-5]. T_{FH} are crucial initiators of the germinal center (GC) response [6,7]. T_{FH} have a distinct developmental pathway characterized by Bcl-6 expression, which is dependent on ICOS

Author Correspondence: Dr. Elizabeth Connick, 12700 E. 19th Avenue, Mail stop B168, Aurora, CO 80045, Liz.Connick@ucdenver.edu, Phone: 303-724-4930, Fax: 303-724-4926.
[2]Current Affiliation, Beacon Clinic, Boulder Community Hospital, 80301

Financial interest statement: The authors claim no conflicts of interests in this study.

Author contributions: BM, DNL, EGR, PJS, and EC designed the experiments. BM, SMM, and MC performed tonsil experiments. BM, JMF, AK, ALM, TA, and MDM performed human lymph node experiments. BM, JMF, EGR, PJS, and EC designed and performed rhesus macaque experiments. BM and EC wrote the manuscript.

expression [8], and produce IL-21 and IL-4 that together optimally drive B cell affinity maturation and antibody specificity [9,10]. ICOS expression on T_{FH} is crucial for both T_{FH} differentiation and immune function [8]. An expansion of T_{FH} cells has been observed in HIV infection [11] and SIV infection [12], yet this expansion does not correlate with improved GC responses. Rather, it has been shown that T_{FH} exhibit impaired activity, partly due to PD-1 ligation, manifested by reduced ICOS expression and inadequate production of IL-21 during HIV infection [13]. It remains unclear whether additional factors may drive the dysregulation of T_{FH} during HIV and SIV infection.

It has recently come to light that B cell follicles contain a novel subset of Treg, termed follicular regulatory T cells (T_{FR}) [14-16]. T_{FR} display a unique transcriptional pattern overlapping that of both T_{FH} and Treg, notably with combined expression of Bcl-6, Foxp3, and Blimp-1. T_{FR} originate from Treg precursors, express CXCR5, and regulate GC responses through interactions with T_{FH} [14-16]. These studies were performed in mouse models, however, and the presence or function of T_{FR} have not yet been described in HIV or SIV infection. Some [17-21], but not all [22-25] studies suggest proportional, not numerical, Treg increases in the peripheral blood of HIV-infected individuals. Studies in lymph nodes and spleen consistently suggest proportional increases of Treg in the context of HIV or SIV infection [26-28], although absolute numbers have not been determined. The impact of Treg on HIV infection is controversial with some studies suggesting that Treg exert a beneficial effect by limiting autoimmunity, HIV replication, and CD4+ T cell depletion [17,18,24,25], while others suggest that Treg have a detrimental effect by inhibiting HIV-specific immune responses and causing disease progression [20,21,28,29]. Although it is reported that Treg from HIV-infected individuals have lower suppressive capacity than those from uninfected individuals [30], it has also been reported that HIV binding to Tregs enhances their suppressive activity and lymphoid homing [31]. Thus, understanding of the role of Treg in HIV infection is still evolving [32], and virtually nothing is known about T_{FR} number and function in HIV infection. Here, we provide evidence for HIV-mediated T_{FR} expansion and the role of T_{FR} in T_{FH} dysregulation during HIV and SIV infection.

Through analyses of secondary lymphoid tissues from chronically HIV-infected humans and chronically SIV-infected rhesus macaques, as well as HIV infection *ex vivo* of human tonsils, we find that T_{FR} are expanded both proportionally and numerically during infection. This expansion is due to a combination of factors, including viral entry and replication, Treg acquisition of CXCR5, TGFβ signaling, T_{FR} proliferation, low apoptosis rates, and increased regulatory dendritic cell (DC) activity. Additionally, we demonstrate that T_{FR} suppress T_{FH} activity during infection by inhibiting T_{FH} proliferation, IL-21 and IL-4 production, and downregulating T_{FH} ICOS expression. The identification of this potent regulator of GC dynamics provides a new therapeutic target for enhancement of anti-viral humoral immunity and vaccine efficacy to promote clearance of HIV.

Results

T_{FR} are increased in chronic HIV and SIV Infections

To determine if T_{FR} were present in human lymphoid tissues, we immunofluorescently labeled lymph node (LN) tissue cross sections from HIV uninfected and HIV-infected

individuals with antibodies to CD4, FoxP3, CD20 and IgD. CD4+Foxp3+ cells were readily detected throughout the LNs including follicular (F), and GC regions, as shown in representative images (Fig. 1a and Supplementary Fig. 1a). Next, we quantified the number of CD4+FoxP3+ cells in total LN, F (CD20+) and GC (CD20+IgD−) regions using 2-3 tissue cross sections per subject. In total LN, the frequencies of CD4+Foxp3+ cells per mm^2 were significantly higher in HIV-infected individuals compared to uninfected controls, but frequencies of CD4+Foxp3+ in F and GC regions did not differ significantly (Fig. 1b). LN enlargement is a hallmark of HIV infection, and therefore frequencies of CD4+FoxP3+ cells per mm^2 underestimate the true differences in absolute numbers of CD4+Foxp3+ cells. The average LN, F, and GC areas in LN cross sections, as determined by quantitative image analysis, were significantly larger in HIV-infected individuals than seronegative individuals (Fig. 1c). We then calculated the number of CD4+Foxp3+ cells per average LN tissue cross-section as well as within each compartment. Absolute numbers of CD4+Foxp3+ cells per average cross-section were significantly increased in HIV-infected individuals compared to HIV-uninfected individuals in all regions (Fig. 1d). The percentage of tissue area that stained positively for CD4 did not differ between HIV seropositive and seronegative individuals, indicating that these individuals had not yet experienced profound CD4 depletion in the lymph node (Supplementary Fig. 1b). In HIV-infected subjects, the percentage of activated (HLA-DR+CD38+) LN CD4+ T cells, as previously determined by flow cytometry [33], did not correlate with number of Treg or T_{FR} and was inversely correlated with GC T_{FR} in the average tissue cross-section (Supplemental Fig. 1c).

To determine if T_{FR} are likewise increased during SIV infection, we analyzed lymphoid cells from uninfected or SIVmac239-infected rhesus macaques by flow cytometry. As SIV infection reduces cell surface CD4, we gated on viable CD3+CD8− cells, as previously described in humans [33]. The surface phenotype of $CD25^{hi}CD127-$ has been shown in humans to encompass Tregs and allow for live cell sorting [34-36]. We validated that this phenotype accurately detects Tregs in SIV-uninfected and SIV-infected rhesus macaques (Fig. 2a). Here, Tregs were defined as viable $CD3+CD8-CD25^{hi}CD127-$, while T_{FR} were defined as the subpopulation that are CXCR5+, and GC T_{FR} as the subpopulation that are $CXCR5^{hi}$ and $PD\text{-}1^{hi}$. In chronic SIV infection, percentages of Tregs, and particularly T_{FR} and GC $T_{FR,}$ were significantly increased compared to SIV-uninfected animals (Fig. 2b). We next determined the ratio of regulatory cell populations to their non-regulatory counterpart and found the ratios of T_{FR} to T_{FH} and GC T_{FR} to GC T_{FH} were significantly higher than those from SIV-uninfected animals, whereas the overall ratio of Treg:non-Treg CD3+CD8− cells did not differ between infected and uninfected animals (Fig. 2c). Treg, T_{FR}, and GC T_{FR} subsets also expressed significantly higher levels of CTLA-4 in SIV-infected compared to SIV-uninfected animals (Fig. 2d).

T_{FR} expansion is mediated by HIV infection

To characterize mechanisms underlying T_{FR} expansion in HIV/SIV infection, we utilized an *ex vivo* model of HIV-1 infection in human tonsil cells. Disaggregated tonsil cells were spinoculated with NL4-3 based X4- or R5-tropic GFP reporter viruses and cultured for 2 days. Productive infection was confirmed by presence of GFP expression after 2 days and percentages of GFP+ T_{FR} ranged from 1-15%. Using the flow gating strategy described

above for rhesus macaques, we demonstrated that $CD25^{hi}CD127-$ cells encompassed the majority of Foxp3+ cells (Fig. 3a). Compared to mock-spinoculated tonsil cells, a 24-hour stimulation of mock-spinoculated tonsil cells with PMA and ionomycin did not significantly increase T_{FR}, whereas the positive control of exogenous TGFβ [37] did (Fig. 3b). A more marked expansion of T_{FR} was observed with either X4- or R5- spinoculation (Fig 3b). Pretreatment of cells prior to spinoculation with chemokine co-receptor antagonists, bicyclam (AMD) for X4 and maraviroc (MVC) for R5, inhibited on average 80% and 86% of productive HIV infection, respectively. Both bicyclam and maraviroc prevented T_{FR} expansion (Fig. 3b). To determine if T_{FR} expansion represented true numerical increases, mock- and X4-spinoculated cultures were analyzed using flow cytometry counting beads.. Total CD3+CD8− cells were decreased and T_{FH} cells were slightly lower 2 days after X4-spinoculation compared to mock-spinoculated cells (Fig. 3c). Conversely, the T_{FR} population was approximately 3-fold higher in X4-spinoculated cells compared to mock-spinoculated cells (Fig. 3c). We further confirmed the phenotype of T_{FR} by determining expression of the transcription factors Bcl-6 and Blimp-1, and evaluated the effects of *ex vivo* HIV-1 infection on their expression. Bcl-6 expression was significantly higher in both T_{FH} and T_{FR} compared to non-follicular (CXCR5−) populations in mock-spinoculated cells at day 2 (Fig. 3d). With X4 or R5 spinoculation, T_{FH} had significantly lower Bcl-6 expression compared to mock-spinoculated cells whereas Bcl-6 expression in T_{FR} was not significantly altered by HIV spinoculation (Fig. 3d). Blimp-1 expression was significantly higher in non-follicular and T_{FR} populations compared to T_{FH} in mock-spinoculated cells at day 2, but was not significantly altered after X4 or R5 spinoculation (Fig. 3e).

IDO and TGFβ production contribute to T_{FR} expansion

To further address viral life cycle contribution to T_{FR} expansion, tonsil cells were treated with the integrase inhibitor raltegravir (RAL) after spinoculation. Raltegravir blocked on average 91% of productive HIV infection and significantly decreased, but did not fully suppress, T_{FR} expansion (Fig. 4a). Additionally, TGFβ is crucial for stable Foxp3 expression in Tregs, so culture supernatants were analyzed for TGFβ production. Stimulation of mock-spinoculated cells with PMA and ionomycin did not lead to increased TGFβ production while the presence of either X4 or R5 virus, even with AMD or MVC pretreatments prior to spinoculation, led to significant increases in TGFβ (Fig. 4b). When tonsil cells were cultured in the presence of TGFβ-neutralizing antibodies, T_{FR} expansion was inhibited in both X4- and R5-spinoculation (Fig. 4c).

Regulatory dendritic cells (DC) are described as myeloid and plasmacytoid DCs that have an immature or semi-mature phenotype and produce anti-inflammatory molecules such as indoleamine 2,3-dioxygenase (IDO) that generates Tregs [38]. It has previously been reported that regulatory DCs inhibit effector T cell function by exhibiting a lack of co-stimulatory molecule expression [39] and can produce IDO in lymphoid tissues during HIV and SIV infection [40-42]. In tonsil cultures, there were significantly more immature myeloid DCs with both X4- and R5-spinoculation, but no significant increase in mature myeloid DCs when compared to mock-spinoculated cells (Fig. 4d). X4- and R5-spinoculation also significantly increased activated plasmacytoid DC compared to mock spinoculation (Fig. 4e). Culture supernatants and lysed cells were then measured for IDO production. There was a

significant increase in IDO with either X4- or R5-spinoculation compared to mock-spinoculation (Fig. 4f). We further analyzed these culture supernatants for IFNγ production, as interferon signaling is upstream of IDO production. X4- and R5-spinoculated cultures tended to have higher levels of IFNγ, but this increase was not statistically significant (Supplementary Fig. 2a).

T_{FR} have high proliferation and low apoptosis rates

In mice T_{FR} arise from conventional Tregs, rather than from T_{FH}[15]. To investigate the origin of T_{FR} in human cells, we evaluated whether tonsil T_{FH} phenotypically converted to T_{FR} or whether Tregs gain CXCR5 expression. T_{FH} (CD3+CD8−CXCR5+CD25−) and non-follicular (CD3+CD8−CXCR5−) T cell populations were sorted and cultured without HIV-spinoculation for 2 days. Interestingly, T_{FH} did not acquire Foxp3 expression, even in the presence of exogenous TGFβ, whereas a small population of cells from the initial CXCR5− population acquired CXCR5 expression (Fig. 5a). These cells, labeled "new" T_{FR}, expressed high levels of Foxp3 (Fig. 5a).

We further hypothesized that cell proliferation may contribute to T_{FR} expansion. We utilized BrdU labeling in tonsil cells to measure the relative rates of T_{FR} and T_{FH} proliferation. Tonsil cells were mock-, X4-, or R5-spinoculated and BrdU DNA incorporation was measured after 2 days by flow cytometry. BrdU incorporation rates were low overall, but in the context of HIV infection, T_{FR} incorporated significantly more BrdU than T_{FH} (Fig. 5b).

To evaluate the duration of tonsil T_{FR} increases, we extended the counting experiments in Fig. 3c for 5 days. Total CD3+CD8−, T_{FH}, and T_{FR} populations from mock-spinoculated samples remained numerically stable up to 5 days (Fig. 5c). In X4-spinoculated samples, total and T_{FH} cells declined by day 5, while T_{FR} were elevated at day 2 and remained so through day 5 (Fig. 5c). We also analyzed cell death rates by Annexin-V and propidium iodide (PI) staining in mock- and X4-spinoculated tonsil cells. Total CD3+CD8− cells and T_{FH} cells displayed increased rates of late apoptosis (Annexin+PI+) and necrosis (PI+) in X4-spinoculated samples compared to mock-spinoculated cells (Fig. 5d). The majority of T_{FR} remained in a state of viability or early apoptosis (Annexin+) in X4-spinoculated tonsil cells, similar to what was seen with mock-spinoculated cells (Fig. 5d). To determine if this occurs during *in vivo* infection, we analyzed Annexin-V staining in disaggregated rhesus macaque lymphoid cells. The levels of Annexin-V staining in total CD3+CD8− and Treg populations were significantly higher in SIV-infected animals compared to SIV-uninfected animals (Fig. 5e). There was not a significant difference in the level of Annexin-V staining in T_{FH} cells in SIV-infection compared to SIV-uninfected animals (Fig. 5e). In contrast, the levels of Annexin-V staining in T_{FR} and GC T_{FR} were significantly lower in SIV-infected animals compared to SIV-uninfected animals (Fig. 5e).

T_{FR} regulatory phenotypes in HIV infection ex vivo

We next sought to determine the regulatory phenotype of tonsil T_{FR} during infection. CTLA-4 and LAG-3 are used to contact and inhibit effector cell function, GITR is expressed on activated and proliferating cells, while galectin receptors are an important family in promoting effector cell apoptosis [43]. Both X4- and R5- spinoculation caused T_{FR} to

significantly upregulate total CTLA-4 (Fig. 6a) and LAG-3 (Fig. 6b), as well as GITR and galectin-3, while galectin-9 expression was not altered (Supplementary Fig. 2b). Regulation of T_{FH} has previously shown to occur through PD-1 ligation [13], however, PD-L1 was expressed on fewer than 3% of T_{FR} following either mock- or X4 spinoculation (n=3). Blockade of chemokine co-receptors partially inhibited CTLA-4 and GITR upregulation on T_{FR} (Fig. 6a and Supplementary Fig. 2a). Blockade of CD4 prior to spinoculation inhibited upregulation of CTLA-4 (Supplemental Fig. 3a) and GITR (Supplemental Fig. 3b) during infection. Blockade of TGFβ led to downregulation of CTLA-4 on T_{FR} during infection (Supplementary Fig. 3c).

IL-10 regulates effector cell function while TGFβ prevents inflammatory responses and promotes Foxp3 expression [43]. IL-10 and TGFβ (LAP-1) production by tonsil T_{FR} was determined by intracellular cytokine staining. Mock-spinoculated cultures treated with exogenous TGFβ as a positive control showed a significant increase of IL-10+ T_{FR} (Fig. 6c). X4- and R5-spinoculation led to significant increases of IL-10+ T_{FR}, which tended to be higher than TGFβ-treated T_{FR} (Fig. 6c). Similar trends were observed in regards to TGFβ+ T_{FR} (Fig. 6d). Additionally, analysis of culture supernatant showed that infection significantly upregulated IL-10 compared to mock-spinoculated controls (Supplementary Fig. 2c), whereas presence of X4 or R5 virus did not significantly increase IL-35 production (Supplementary Fig. 2d).

T_{FR} dysregulate T_{FH} activity

T_{FR} have been shown to modulate T_{FH} function and thereby control GC reactions in mice [14-16]. Given that T_{FH} exhibit impaired function in chronic HIV infection [13] we investigated whether T_{FH} were impaired by T_{FR} in the tonsil model. We first compared the expression of ICOS, a key molecule for T_{FH} maintenance and function, in X4- or R5-spinoculation to mock-spinoculation. With both X4- and R5-spinoculation, T_{FH} demonstrated a significant reduction of ICOS expression (Fig. 7a). We evaluated the role of Tregs in T_{FH} ICOS downregulation by depleting CD25+ regulatory cells, which effectively removes all Foxp3+ cells from tonsil cell culture, and analyzing T_{FH} after 2 days. ICOS expression on T_{FH} was high in mock-spinoculated controls regardless of presence or absence of Treg (Fig. 7b). With X4- or R5-spinoculation, however, ICOS expression was not downregulated when Tregs were absent (Fig. 7b). While CD25+ cell depletion effectively removes overall regulatory populations, we could not rule out that T_{FR} may have functions differing from those of Tregs. We therefore examined the regulatory effects of T_{FR} specifically by isolating tonsil T_{FH} and adding T_{FR} back to T_{FH} at increasing ratios. In X4- and R5-spinoculated cultures, we observed that T_{FH} ICOS levels were decreased as the ratio of T_{FR} increased (Fig. 7c).

Previous studies using *ex vivo* suppression assays have shown that Treg inhibit CD4+ T cell proliferation and cytokine production in HIV infection [18,21]. First, we investigated the ability of T_{FR} to suppress proliferation of T_{FH} in the context of *ex vivo* HIV infectionTonsil T_{FH} and T_{FR} were isolated, spinoculated with either X4 or R5 virus, and cultured either alone or with equal numbers of T_{FR} for 4 days in the presence of anti-CD3/anti-CD28

antibodies and IL-2. T_{FR} consistently inhibited proliferation of T_{FH} in both X4- and R5-spinoculated cultures (Fig. 7d).

Next, we investigated the role of T_{FR} on T_{FH} cytokine production. Initially, we observed that tonsil T_{FH} display decreased IL-4 production in either X4- or R5-spinoculated cultures, while IL-21 production did not have a uniform trend (Supplemental Fig. 4a). Removal of CD25+ Tregs led to significant increases in IL-4 (Fig. 8a) and IL-21 (Fig. 8b) production by tonsil T_{FH} following mock-, X4-, and R5-spinoculation and significant increases in IL-4 and IL-21 production by T_{FH} in both uninfected and chronically SIV-infected animals (Fig. 8c). We further validated these observations by co-culturing tonsil T_{FH} with increasing ratios of T_{FR} following spinoculation with X4 virus. The absence of T_{FR} led to increased T_{FH} production of IL-4 and IL-21 (Fig. 8d). The regulation of T_{FH} was T_{FR} dose-dependent, as an increasing ratio of T_{FR} led to increasing inhibition of T_{FH} IL-4 and IL-21 production (Fig. 8d). To determine if the suppressive capacity of T_{FR} was due to the production of suppressive cytokines, we performed intracellular cytokine assays in the presence of both IL-10 and TGFβ neutralizing antibodies. Previous reports show that IL-10 potently blocks IL-4 production [44], so we specifically addressed IL-21 production by T_{FH}. Neutralization of IL-10 and TGFβ restored some, but not the majority of IL-21 production by T_{FH} in the presence of T_{FR} (Fig. 8e).

Discussion

In the present study, we provide a comprehensive analysis of T_{FR} in HIV and SIV infection. We show that T_{FR} are expanded in secondary lymphoid tissues during both chronic HIV and SIV infection. In addition, we utilize HIV infection *ex vivo* to show that cell proliferation, regulatory dendritic cells, TGFβ signaling, Treg acquisition of CXCR5, and resistance to apoptosis play a role in T_{FR} expansion. Finally, we demonstrate that T_{FR} are able to inhibit proliferation, ICOS expression, and IL-4 and IL-21 production by T_{FH}. Collectively, these findings reveal that T_{FR} play a crucial role in the impairment of T_{FH} during HIV and SIV infection.

Although Tregs are diminished in gut-associated lymphoid tissue during HIV infection [23], prior studies indicate an increase in Tregs in lymph nodes [21,26,45]. We found that absolute numbers of CD4+FoxP3+ cells in follicles and germinal centers per average lymph node cross section were increased in HIV-infected individuals compared to uninfected individuals. Furthermore, following *ex vivo* infection of human tonsil cells, we demonstrated that T_{FR} increase both proportionally and numerically. As Foxp3 can be transiently upregulated after T cell activation, we evaluated whether percentages of activated cells were related to Foxp3 expression. Nevertheless, we found no correlation between percentages of activated lymph node cells and Tregs and T_{FR}, and numbers of GC T_{FR} were inversely related to percentages of HLA−DR+CD38+CD4+ cells, which is the opposite of what would expect if immune activation was driving Foxp3 expression.

Blockade of the HIV chemokine co-receptors CXCR4 and CCR5 prevented T_{FR} expansion in tonsil cells, thus demonstrating that viral entry was necessary to promote expansion. Intriguingly, however, treatment with the integrase inhibitor raltegravir, which blocks the

virus replication cycle after cell entry, largely blunted but did not completely ablate T_{FR} expansion. It has recently been demonstrated that many cells during *ex vivo* HIV infection are abortively infected and only a minority of infected cells are productively infected [46]. As HIV-producing T_{FR} were a minor population of T_{FR} overall, our findings suggest that abortive infection of T_{FR} cells alone could induce some T_{FR} expansion. Viral sensing mechanisms are important for innate immune cell activation in HIV infection and similar mechanisms may also contribute to T_{FR} activation and proliferation. HIV RNA sensing through internal TLR7 activates pDC [47] and TLR7 ligation has been shown to induce CD4 T cell proliferation [48]. It is possible that HIV sensing by T_{FH} or T_{FR} contributes to T_{FR} expansion and further studies concerning abortive and productive infections are warranted. It has been reported that Treg increases in untreated HIV-infected individuals are diminished after treatment with antiretroviral therapy (ART), but do not normalize [49]. A recent study demonstrated that addition of maraviroc to ART regimens led to further reductions in Tregs in individuals who were already virologically suppressed [50]. These data, in conjunction with our findings, suggest that in HIV-treated individuals who are fully suppressed on ART regimens that do not include maraviroc, ongoing nonproductive HIV infection or a low level of HIV replication is occurring resulting in persistent T_{FR} expansions that may contribute to immune impairments.

Tonsil T_{FR} increased their regulatory capacity during X4 or R5 HIV infection, as evidenced by increased CTLA-4, LAG-3, GITR, and galectin-3 expression and production of IL-10 and TGFβ. In contrast to T_{FR} expansions, however, the increased regulatory phenotype was only partially reduced by the addition of bicyclam and maraviroc, but fully reduced by CD4 blockade. This finding is consistent with the observation that HIV binding to CD4 molecules enhances their regulatory phenotype and suppressive capabilities [31]. Additionally, we found that blockade of TGFβ signaling fully inhibited T_{FR} regulatory phenotype enhancement during HIV infection. Importantly, we found almost no expression of PD-L1 by tonsil T_{FR}, suggesting that this regulatory molecule does not mediate their effects on T_{FH}. Dissecting out the distinct mechanisms responsible for expansion and enhanced regulatory profiles of T_{FR} in HIV infection could identify potential therapeutic targets to suppress excessive T_{FR} activity and could have relevance to host-pathogen interactions in other diseases as well.

We also investigated whether intrinsic characteristics of T_{FR} might promote their expansion during HIV infection. We found significant increases in cell proliferation of tonsil T_{FR} compared to tonsil T_{FH} during both X4 and R5 HIV infection. It has been well-established that regulatory DCs induce Tregs in HIV infection, and exert this effect in part by low rates of maturation and co-stimulatory molecules [39] and in part by IDO production [40,51]. The lack of DC maturation observed during HIV infection could contribute to increased Treg and T_{FR} [52]. In tonsil cells, we found that myeloid DCs were mostly immature, while activated plasmacytoid DC were significantly increased in HIV infection, which recapitulates previous studies in HIV [39,53,54] and SIV [41,42] infection *in vivo*. Tonsil cell cultures also exhibited increased levels of IDO, the IDO upstream activator IFNγ, and TGFβ during HIV infection. Type I interferons were not specifically studied in this work, but they have also shown to be increased in tonsil cells infected with NL4-3 HIV virus [55]. These factors present

in the follicular milieu likely contribute to enhanced proliferation and numerical increases of T_{FR}.

HIV-infected individuals have high rates of overall CD4+ T cell apoptosis [56] and higher levels of Annexin-V binding and caspase-3 activation in Tregs compared to uninfected controls [29]. We similarly found that total CD3+CD8− cells and Tregs had higher levels of Annexin-V binding in chronically SIV-infected rhesus macaques. Remarkably, however, we found that $T_{FR,}$ GC $T_{FR,}$ and GC T_{FH} had lower levels of Annexin-V binding in SIV-infected rhesus macaques compared to uninfected animals. Furthermore, T_{FR} and GC T_{FR} had the lowest levels of Annexin-V binding of any subset in SIV-infected macaques, but not in uninfected macaques. These findings imply that regulatory follicular cells may be more resistant to apoptosis than other subsets, which could promote their accumulation. This could explain our observation that lymphoid tissue ratios of T_{FR} to T_{FH} and GC T_{FR} to GC T_{FH} in chronically SIV-infected rhesus macaques were significantly higher than those from SIV-uninfected animals, but that this phenomenon was not observed in the Treg population as a whole compared to non-Treg CD3+CD8− cells. We recently reported that tonsil follicular CD4+ T cells have elevated Bcl-2 expression and Bcl-2 is further upregulated on cells that are productively infected with R5 virus [57]. These studies did not discriminate between T_{FR} and T_{FH} populations, however. Thus, elevated Bcl-2 expression on T_{FR} could be a mechanism that protects T_{FR} from apoptosis. The mechanisms of T_{FR} apoptosis and how they contribute to T_{FR} number warrant further investigation.

In characterizations of T_{FR} in mice, it was shown that T_{FR} arise from non-T_{FH} precursors and express both Blimp-1 and Bcl-6 [14,15]. To assess this in humans, we isolated both T_{FH} and non-follicular (CXCR5−) subsets from tonsils and looked for alterations in their phenotype. T_{FH} did not acquire a T_{FR} phenotype, even when provided with exogenous TGFβ. A small population of CXCR5− cells, however, acquired CXCR5 expression and expressed Foxp3. Despite being numerically small, this new T_{FR} population could contribute substantially to increase the T_{FR} population. Intriguingly, it was recently shown that T_{FH} differentiation and maintenance was optimized by TGFβ in combination with T_{FH} cytokines IL-12 and IL-23, but naïve CD4+ T cells cultured with TGFβ alone acquired Treg expression profiles while promoting CXCR5 expression [58]. This further supports the notion that the expansions of T_{FR} observed in our study likely originate from non-T_{FH} precursors. We also find that human T_{FR} express Bcl-6 and Blimp-1 and neither was altered after HIV spinoculation. However, expression of Bcl-6 by T_{FH} was significantly reduced after HIV spinoculation. A more detailed analysis would be valuable to reveal the effects of HIV on both T_{FH} and T_{FR} transcriptional profiles.

A hallmark of HIV infection is the production of high levels of HIV-specific antibodies that are unable to suppress HIV [27]. HIV-specific neutralizing antibodies are produced in many individuals during HIV infection [59], however the virus is able to rapidly mutate and avoid recognition [60,61]. Although broadly neutralizing antibodies (bNabs) are effective in suppressing HIV replication [62], few people develop bNabs [63]. Whether T_{FR} limit the ability of HIV-infected individuals to develop bNabs is an important question. BNabs are characterized by high affinity maturation rates in GCs, and functional T_{FH} are crucial for somatic hypermutation levels of maturing B cells in follicles [6]. The level of bNabs in a

cohort of HIV seronegative individuals who received an HIV vaccine positively correlated to functional circulating resting memory T_{FH} [64]. We demonstrate that T_{FR} inhibited the ability of T_{FH} to proliferate, to produce crucial B cell help cytokines IL-4 and IL-21, and maintain ICOS expression. Whether these factors are key to developing bNabs is of critical importance to address. Apart from direct effects on T_{FH}, T_{FR} may inhibit bNab production through direct interactions with B cells, or indirectly by altering the follicle microenvironment or follicular DC network during HIV infection. Thus, understanding the impact of T_{FR} on the germinal center reaction and development bNabs is complex. These questions cannot be readily addressed within tissue cultures systems, but would be best answered in an interventional study in which T_{FR} are manipulated.

The dynamics of GC formation in acutely SIV-infected rhesus macaques were recently characterized [65]. Interestingly, animals with the most impaired GC development experienced the most rapid disease progression. It would be important to evaluate whether a robust T_{FR} response correlates with the greatest impairment in GC formation in these animals. Interestingly, Treg-depleted mice infected with influenza had limited GC size and compromised influenza-specific T_{FH} responses [66]. One possible explanation is that T_{FR} are critical for GC formation and fine-tuning of immune responses during acute infections, but may exert more suppressive responses in chronic disease [67]. It will be important to determine the precise role of T_{FR} in GC development and maintenance during different stages of HIV, as well as in other chronic infections.

T_{FR} are emerging as important drivers of GC dynamics. Our findings that T_{FR} are expanded during HIV infection and impair T_{FH} function have multiple important implications. First, they provide a potential mechanism for the impaired humoral responses observed in untreated HIV-infected individuals, particularly the inability to develop bNabss. Secondly, they provide a potential explanation for persistent impairments in humoral immunity seen in HIV-infected individuals, despite good virologic suppression on ART that does not contain a CCR5 receptor blocker. They further suggest that prophylactic HIV vaccines should be designed to minimize induction of T_{FR}, as they could impair development of protective antibody responses. Finally, these studies have implications for diseases and vaccine strategies apart from HIV infection, as it is likely that T_{FR} play a key role in immune responses to many infections. Thus, a better understanding of the role of T_{FR} in the context of HIV infection can provide important insights into the dynamics of germinal center responses and humoral immunity during infection and adds a new dimension to the intricacies of vaccine development.

Methods

Human and rhesus macaque subjects and clinical specimens

Inguinal lymph nodes were obtained by excisional biopsy in an outpatient procedure as previously described [4] from individuals with documented HIV-1 infection for at least 6 months, who were not receiving antiretroviral therapy and had $CD4^+$ T-cell counts of $\geq 300/mm^3$. None of these subjects had an opportunistic infection, malignancy, or acute illness at the time of lymph node excision. CD4+ T cell counts ranged from 214 to 1103 cells/mm^3 (median, 478 cells/mm^3), and plasma viral load ranged from 2.87 to 5.88 $\log_{10}$

copies/ml (median, 4.26 $\log_{10}$ copies/ml). A total of 10 (53%) of subjects were females, ages ranged from 21 to 50 years (median, 34 years), and 10 (53%) were white including 3 Hispanics, and 9 were black (47%). Inguinal lymph nodes were also obtained from HIV-1-seronegative individuals while they underwent a non-emergent surgical procedure in the groin area. A total of 6 (75%) of seronegative subjects were female, ages ranged from 32 to 71 years (median, 50 years), and 7 (88%) were white including one Hispanic, and one (12%) was black. Informed consent was obtained from all lymph node donors. Human tonsils were obtained from the Colorado Children's Hospital (Aurora, Colorado, USA) following routine tonsillectomy from individuals at low risk for HIV infection. Use of tonsil specimens for these studies was reviewed by the Colorado Multiple Institutional Review Board and determined to not constitute human subjects research, in accordance with guidelines issued by the Office of Human Research Protections (http://www.hhs.gov/ohrp/policy/checklists/decisioncharts.html), and consequently, informed consent was not required. All research involving human subjects conformed to the principles set forth in the Declaration of Helsinki and was approved by the Colorado Multiple Institutional Review Board. Lymph nodes and spleen were obtained from SIVmac239-infected and uninfected Indian rhesus macaques (*Macaca mulatta*). Animals were infected either intravenously or intrarectally with SIVmac239, and had been infected from 12 to 241 weeks (median, 19.5 weeks) at the time that specimens were obtained. Plasma SIV RNA concentrations ranged from 3.77 to 6.76 $\log_{10}$ copies/ml (median, 5.72 $\log_{10}$ copies/ml), and CD4+ T cell counts ranged from 142 to 569 cells/mm^3 (median, 348 cells/mm^3). Of SIV-infected animals, 4 (40%) were female and they ranged in age from 7 to 17 years (median, 9 years). Of SIV uninfected animals, 2 (22%) were female and they ranged in age from 3 to 23 years (median, 4 years). Animals were housed and cared for in accordance with American Association for Accreditation of Laboratory Animal Care standards in accredited facilities, and all animal procedures were performed according to protocols approved by the Institutional Animal Care and Use Committees of the Wisconsin National Primate Research Center. Tissues were either shipped overnight on ice in cold RPMI 1640 and disaggregated, or disaggregated at the Wisconsin National Primate Research Center and frozen cells shipped on liquid nitrogen to the University of Colorado. Sample sizes in this study were based on upon availability of specimens and prior experience of the necessary sample size to see anticipated effects.

Quantification of Foxp3+CD4+ cells in lymphoid tissues

Six-micrometer frozen sections of LN were thaw mounted onto slides and fixed in 1% paraformaldehyde (Sigma) in PBS. Two or three sections, at least 60 μm apart, were stained and evaluated for each subject. Indirect immunofluorescent staining was performed by first staining with Rabbit anti-IgD (Novus, cat# NB120-17184, 1:50, Littleton, CO) and mouse anti-Foxp3 (clone 236A/E7; eBiosciences, cat#14-4777-82, 1:100, San Diego, CA) for 1 hour followed by detection with Pacific Blue anti-Rabbit IgG (cat# P10994, 1:100) and AF488 anti-mouse IgG (cat#A21200, 1:200) (both from Invitrogen, Grand Island, NY) for 30 min. After washing, sections were incubated for an additional hour with Rabbit anti-CD20 (Abcam, cat# ab27093, 1:400, Cambridge, MA) and Rat anti-CD4 (clone YNB46.1.8; AbD Serotec, cat# MCA484G, 1:100, Raleigh, NC) followed by detection with AF647 anti-rabbit IgG (Invitrogen, cat#A21443, 1:200) and AF594 anti-rat IgG (Invitrogen, cat#A21209, 1:200). Slides were covered with coverslips using SlowFade Gold (Invitrogen).

Images of full sections were generated at 60X using an Olympus VS120 scanner outfitted with an OrcaR2 camera (Olympus, Center Valley, PA). Ten random images were extracted for each section from the main scans and Foxp3+CD4+ cells/mm^2 of total, follicle (CD20+) and GC (CD20+IgD−) was determined using visual inspection and quantitative image analysis (Qwin Pro 3.4.0, Leica Microsystems, Wetzlar, Germany). The areas of each lymph node cross section, as well as the follicular and GC compartments were determined by quantitative image analysis and averaged for each subject. The average number of FoxP3+CD4+ cells per LN cross section and compartment was calculated by multiplying the frequency of FoxP3+CD4+ cells by the average area of the LN, follicle or GC in each subject.

Quantitation of activated CD4+ T cells in human lymph nodes

Disaggregated lymph node cells (5×10^6) were stained with antibodies to CD3-PEcy5-UCHT1 (BD Biosciences, San Jose, CA 555334), CD4-APC-H7-RPAT4 (BD 560158), CD38-FITC-240742 (Invitrogen FAB2404F), and HLA-DR-APC-L243 (BD 340549), evaluated by flow cytometry (LSR II, BD Immunocytometry Systems), and analyzed using FlowJo (Tree Star, Ashland, OR). All antibodies were used at one test per 10^6 cells.

HIV reporter viruses and tonsil infection model

The HIV-1 NL4-3-based CXCR4 (X4)-tropic green fluorescent protein (GFP) reporter virus NLENG1-IRES [68] and the CCR5 (R5)-tropic GFP reporter virus NLYUV3-GFP [33] were used for tonsil cell infections. Virus stocks were prepared by transfecting 293T cells with either X4 or R5 plasmid constructs (Effectine, Qiagen) in complete DMEM (DMEM + 10% FBS, pen/strep, and non-essential amino acids), collecting supernatants, and spinning at 800 × *g* to remove debris. Viral stocks were stored at −80 °C prior to use. After disaggregation, 5×10^6 tonsil cells were spinoculated with either GFP reporter virus or a mock spinoculation with an equal volume of complete DMEM for 2 hours at 1200 × *g* at room temperature. Cells were washed to remove unbound virus and media, and cultured for 2 days at 37 °C with 5% CO_2 in RPMI with 10% FBS, L-glutamine, and pen/strep (R10) at a density of 1.5×10^6 cells/mL. To block viral entry, tonsil cells were incubated in R10 at 37 °C with 5% CO_2 for 1 hour with 2 μM maraviroc, 200 μM bicyclam, or 10 ng/mL of anti-human CD4 (BioLegend 300515). To block HIV replication, tonsil cells were incubated with 10 μM of the integrase inhibitor raltegravir in R10 for 1 hour prior to spinoculation and included in the culture for 2 days. To block TGFβ signaling, 2 μg/mL of anti-human TGFβ (BioLegend 521703) was included for the duration of the culture. Exogenous TGFβ (Sigma T7039) was added at 100 ng/mL in select cultures as a positive control to induce Treg and T_{FR}. At the end of culture, the cell supernatants were collected, centrifuged at 6800 × *g* to remove debris, and frozen at −80 °C for subsequent ELISA analysis. Cells were collected and immediately processed for analysis by flow cytometry.

Flow cytometry analysis of T cells and dendritic cells

Cells were blocked for 20 minutes with 2% BSA in PBS at 4 °C and then stained for 30 minutes at 4 °C in the dark. For T cell phenotyping, the following anti-human conjugated antibodies were used: CD3-APCCy7-UCHT1 (Tonbo 25-0038), CD8-eVolve605-RPA-T8

(eBioscience 83-0088), CD25-PECy7-BC96 (Tonbo 60-0259), CXCR5-PE-MU5UBEE (eBioscience 18-9185), CD127-Pacific Blue-A1095 (BioLegend 351306), ICOS-ISA-3 (PECy7 or APC) (BioLegend 313520, 313510), PD-1-APC-MIH4 (eBioscience 17-9969) or PD-1-APC-EH12.2H7 (BioLegend 329908), Bcl6-PerCPCy5.5 -K112-91 (BD 562198), Blimp1-646702 (R&D IC36081A), CTLA-4-PerCPeFluor710-14D3 (eBioscience 46-1529), GITR-PE-eBioAITR (eBioscience 12-5875), LAG-3-APC-3DS223H (eBioscience 17-2239), Galectin-3- AF647-M3/38 (Biolegend 125408) and Galectin-9-PerCPCy5.5-9M1-3 (BioLegend 348910). The same panel was used for rhesus macaque cell staining with the single exception of CD3-APCCy7-SP34-2 (BD 557757). Foxp3 expression in CD25+CD127− cells was confirmed using Foxp3-PE-PHC1O1 and the Foxp3/ Transcription factor permeabilization kit (eBioscience 72-5776) according to manufacturers' protocols. For dendritic cell phenotyping, the following anti-human conjugated antibodies were used: CD14-eFluor450-61D3 (eBioscience 8048-0149), CD1c-PECy7-L161 (eBioscience 25-0015), CD3-APCCy7-UCHT1 (Tonbo 25-0038), CD11c-PE-3.9 (eBioscience 12-0116), CD19-AF700-HIB19 (BioLegend 302226), CD83-BV510-HB15e (BD 563223), CD123-BV605-7G3 (BD 564197), DC-SIGN-PerCPCy5.5-eB-h209 (eBioscience 45-2099) and HLA-DR-APC-L243 (BD 340691). All analyses were performed on Aqua LIVE/DEAD (Molecular Probes L34957) or Ghost Dye 510 (Tonbo 13-0870) negative cells. Fresh human tonsil cells were typically 70-90% viable after culture and cryopreserved rhesus macaque cells ranged from 40-80% viability after freeze/thaw. All antibodies were used at one test per 10^6 cells. Cells were fixed with 2% paraformaldehyde. Data were acquired on a custom LSR II flow cytometer (Serial # H47100196, BD Immunocytometry System, San Jose, CA) with BDFACS Diva (v6.1) and with a configuration of 6 filters (755LP, 685LP, 670LP, 635LP, 600LP, 550LP, and 505LP) on a blue laser (488 nm), 3 filters (595LP, 505LP, and 450/50) on a violet laser (405 nm), and 3 filters (755LP, 685LP, and 670/30) on a red laser (633 nm). FCS files were analyzed using FlowJo (v10.7, Tree Star, Ashland, OR).

T_{FR} counts and cell death time course

For the 5-day time course, cells were prepared and cultured as above with the exception of addition of 10 U/mL of IL-2 to culture. Cells were harvested and analyzed each day for cell death and total counts. Cell counts were performed using CountBright absolute counting beads (Molecular Probes C36950) according to manufacturers' instructions. Briefly, all cell fractions were resuspended in 400 μL of buffer and 50 μL of beads were added. At least 1,000 bead events were collected for each sample and the number of cells/ μL was calculated based on the fixed bead concentration supplied by the manufacturer. In addition, a separate analysis of the same cell fractions was performed using the Annexin-V PE apoptosis detection kit (eBioscience 88-8102) according to the manufacturers' instructions. Each T cell population was analyzed based on early apoptosis (Annexin-V staining), late or advanced apoptosis (Annexin-V and propidium iodide), and necrosis (propidium iodide).

ELISAs

Cell culture supernatants were measured for TGFβ-1 secretion (R & D systems DB100B), IL-10 (R & D systems DB1000B), IFNy (R & D systems DIF50) and indoleamine 2,3-dioxygenase (IDO, Cloud Clone SEB547Hu) according to manufacturer's instructions.

Absorbance values were converted to protein levels using a protein standard dilution. Cell lysates as well as culture supernatants were evaluated by IDO ELISA.

Intracellular Cytokine Staining assays

After 2 days of culture, tonsil cells were stimulated with 50 ng/mL of phorbol 12-myristate 13-acetate (PMA, Sigma P8139) and 1 μg/mL of ionomycin (Sigma I3909) in the presence of protein transport inhibitor containing monensin (BD GolgiStop) for 5 hours. Cryopreserved rhesus macaque cells were rested for 24 hours (viability 40-80%) in R10 and then stimulated in the same manner for 5 hours. Cells were then harvested, blocked and stained for surface markers as above, and then fixed and permeabilized using BD CytoFix/Cytoperm kit (554714) according to manufacturers' instructions. Cells were then stained at 4 °C for 30 minutes with IL-4-PercpCy5.5-8D4-8 (BD 561234), IL-10-eFluor450-JES3-9D7 (eBioscience 48-7108), IL-21-AF647-3A3-N2.1 (BD 560493), and TGFβ-1-PE(LAP)-27232 (R&D FAB2463P). All antibodies were used at one test per 10^6 cells. All cytokine analyses were normalized to a mock-spinoculated control that received monensin but was unstimulated.

CD25-depletion cultures

CD25+ cells were depleted immediately after tonsil cell disaggregation using a FITC positive selection kit (StemCell 18558) and CD25-FITC-BC96 (Biolegend 302604). Cells were spinoculated and cultured as described above. Mock- and HIV-spinoculated cultures from non-depleted cells were run in parallel with each experiment. After 2 days of culture, cells were analyzed for T_{FH} and T_{FR} phenotypes by flow cytometry as described above. A subset of CD25+ depleted cells was analyzed to confirm the absence of Foxp3+ cells.

BrdU ex vivo proliferation assay

Ex vivo BrdU labeling was performed using a flow cytometry kit (eBioscience 8817-6600) according to manufacturers' instructions. For BrdU labeling of primary cells in culture, a range of incubation times for BrdU uptake were tested and 24 hours was found to be the optimal. Tonsil cells were spinoculated and cultured as above and labeled with 10 μM of BrdU for 24 hours prior to analysis. After 2 days of culture, cells were collected, stained with surface antigens, fixed and permeabilized, and treated with DNase I to allow BrdU antibody binding.

Cell sorting and T_{FR}/T_{FH} co-culture

Disaggregated tonsil cells were sorted using a MoFlo Astrios EQ. Cells were sorted into non-follicular (CD3+CD8−CXCR5−), T_{FH} (CD3+CD8−CXCR5+CD25−), and T_{FR} (CD3+CD8−CXCR5+CD25hi) populations. A subset of non-follicular and T_{FH} cells were cultured either without treatment or with 100 ng/mL of exogenous TGFβ to analyze whether T_{FH} convert to T_{FR}. After sorting, T_{FH} and T_{FR} were spinoculated with X4 or R5 HIV GFP reporter viruses. T_{FH} were then seeded at a set number of 1×10^5 cells in a 24 well plate and T_{FR} were added at ratios of 1:1, 1:10, and 1:50. After 2 days, cells were stimulated to measure IL-4 and IL-21 by ICS or left unstimulated to measure ICOS expression. In select

experiments, T_{FH} and T_{FR} were co-cultured in the presence of IL-10 (1 ug/mL Biolegend 501406) and TGFβ (1ug/mL Biolegend 521704) neutralizing antibodies.

Proliferation assays

T_{FH} (CD3+CD8−CXCR5+CD25−) were sorted and stained with proliferation dye (Cell Proliferation Dye eFluor670, eBioscience 65-0840) at a concentration of 0.5 μM. In a 96-well plate, pre-coated with 5 μg/mL anti-CD3 (Tonbo 40-0037) in PBS at 37°C for 2 hours, 10^4 T_{FH} per well were cultured for 4 days in 200 μL R10 containing 2 μg/mL anti-CD28 (Tonbo 40-0289) and 10 U/mL IL-2 with an equal number of sorted T_{FR} (CD3+CD8−CXCR5+ CD25+CD127−) or alone. At day 4, cells were stained with viability dye (Ghost V450, Tonbo 13-0863) and analyzed by flow cytometry.

Statistical analysis

Comparisons of infected and seronegative human lymph nodes or rhesus macaque spleen or lymph nodes were performed by non-parametric Mann Whitney tests. Comparisons of tonsil cultures were performed by unpaired Mann Whitney or Friedman nonparametric tests. In direct comparisons of paired data, a paired Wilcoxon ranked sums test was performed to compare the two group medians of interest. Significance is denoted in each figure by asterisks, as * = $p < 0.05$, ** = $p < 0.01$, and *** = $p < 0.001$.

Supplementary Material

Refer to Web version on PubMed Central for supplementary material.

Acknowledgements

The authors would like to thank Mario Santiago for valuable discussions and comments. The authors would also like to thank David Watkins and Nancy Wilson for sharing reagents and animal specimens. Maraviroc (cat #11580), bicyclam (cat # 8128), and raltegravir (cat # 11680) were obtained through the NIH AIDS reagent program. This work was funded by NIH/NIAID grants R01 AI096966 to E.C. and P.S., 5T32AI007447-22 T32 to B.M., T32 5T32AI007447 to M.C., T32 AI007405 to S.M, and the Wisconsin National Primate Research Center (WNPRC) P51OD011106. Cell sorting was performed by the University of Colorado Cancer Flow Cytometry Shared Resource, which is supported by the Cancer Center Support Grant P30CA046934 and the Skin Diseases Research Cores Grant P30AR057212. The funding source played no role in experimental design or data analysis.

References

1. Chomont N, et al. HIV reservoir size and persistence are driven by T cell survival and homeostatic proliferation. Nat Med. 2009; 15:893–900. doi:http://www.nature.com/nm/journal/v15/n8/suppinfo/nm.1972_S1.html. [PubMed: 19543283]
2. Schacker T, et al. Rapid accumulation of human immunodeficiency virus (HIV) in lymphatic tissue reservoirs during acute and early HIV infection: implications for timing of antiretroviral therapy. Journal of Infectious Diseases. 2000; 181:354–357. [PubMed: 10608788]
3. Perreau M, et al. Follicular helper T cells serve as the major CD4 T cell compartment for HIV-1 infection, replication, and production. The Journal of experimental medicine. 2013; 210:143–156. [PubMed: 23254284]
4. Folkvord JM, Armon C, Connick E. Lymphoid follicles are sites of heightened human immunodeficiency virus type 1 (HIV-1) replication and reduced antiretroviral effector mechanisms. AIDS Research & Human Retroviruses. 2005; 21:363–370. [PubMed: 15929698]
5. Pantaleo G, et al. Lymphoid organs function as major reservoirs for human immunodeficiency virus. Proceedings of the National Academy of Sciences. 1991; 88:9838–9842.

6. Crotty S. Follicular helper CD4 T cells (Tfh). Annual review of immunology. 2011; 29:621–663.
7. Chtanova T, et al. T follicular helper cells express a distinctive transcriptional profile, reflecting their role as non-Th1/Th2 effector cells that provide help for B cells. The Journal of Immunology. 2004; 173:68–78. [PubMed: 15210760]
8. Choi YS, et al. ICOS receptor instructs T follicular helper cell versus effector cell differentiation via induction of the transcriptional repressor Bcl6. Immunity. 2011; 34:932–946. [PubMed: 21636296]
9. Linterman MA, et al. IL-21 acts directly on B cells to regulate Bcl-6 expression and germinal center responses. The Journal of experimental medicine. 2010; 207:353–363. [PubMed: 20142429]
10. Eto D, et al. IL-21 and IL-6 are critical for different aspects of B cell immunity and redundantly induce optimal follicular helper CD4 T cell (Tfh) differentiation. PloS one. 2011; 6:e17739. [PubMed: 21423809]
11. Lindqvist M, et al. Expansion of HIV-specific T follicular helper cells in chronic HIV infection. The Journal of Clinical Investigation. 2012; 122:3271–3280. doi:10.1172/JCI64314. [PubMed: 22922259]
12. Petrovas C, et al. CD4 T follicular helper cell dynamics during SIV infection. The Journal of clinical investigation. 2012; 122:3281–3294. [PubMed: 22922258]
13. Cubas RA, et al. Inadequate T follicular cell help impairs B cell immunity during HIV infection. Nat Med. 2013; 19:494–499. doi:http://www.nature.com/nm/journal/v19/n4/abs/nm.3109.html#supplementary-information. [PubMed: 23475201]
14. Chung Y, et al. Follicular regulatory T cells expressing Foxp3 and Bcl-6 suppress germinal center reactions. Nature medicine. 2011; 17:983–988.
15. Linterman MA, et al. Foxp3+ follicular regulatory T cells control the germinal center response. Nature medicine. 2011; 17:975–982.
16. Wollenberg I, et al. Regulation of the germinal center reaction by Foxp3+ follicular regulatory T cells. The Journal of Immunology. 2011; 187:4553–4560. [PubMed: 21984700]
17. Card CM, et al. Decreased immune activation in resistance to HIV-1 infection is associated with an elevated frequency of CD4+ CD25+ FOXP3+ regulatory T cells. Journal of Infectious Diseases. 2009; 199:1318–1322. [PubMed: 19301980]
18. Kinter AL, et al. CD25+ CD4+ regulatory T cells from the peripheral blood of asymptomatic HIV-infected individuals regulate CD4+ and CD8+ HIV-specific T cell immune responses in vitro and are associated with favorable clinical markers of disease status. The Journal of experimental medicine. 2004; 200:331–343. [PubMed: 15280419]
19. Lim A, et al. Proportions of circulating T cells with a regulatory cell phenotype increase with HIV-associated immune activation and remain high on antiretroviral therapy. Aids. 2007; 21:1525–1534. [PubMed: 17630546]
20. Suchard MS, et al. FOXP3 expression is upregulated in CD4+ T cells in progressive HIV-1 infection and is a marker of disease severity. PLoS One. 2010; 5:e11762. [PubMed: 20668701]
21. Weiss L, et al. Human immunodeficiency virus–driven expansion of CD4+ CD25+ regulatory T cells, which suppress HIV-specific CD4 T-cell responses in HIV-infected patients. Blood. 2004; 104:3249–3256. [PubMed: 15271794]
22. Epple H-J, et al. Mucosal but not peripheral FOXP3+ regulatory T cells are highly increased in untreated HIV infection and normalize after suppressive HAART. Blood. 2006; 108:3072–3078. [PubMed: 16728694]
23. Angin M, et al. Preserved function of regulatory T cells in chronic HIV-1 infection despite decreased numbers in blood and tissue. Journal of Infectious Diseases. 2012; 205:1495–1500. [PubMed: 22427677]
24. Eggena MP, et al. Depletion of regulatory T cells in HIV infection is associated with immune activation. The Journal of Immunology. 2005; 174:4407–4414. [PubMed: 15778406]
25. Montes M, et al. Foxp3+ regulatory T cells in antiretroviral-naive HIV patients. Aids. 2006; 20:1669–1671. [PubMed: 16868450]
26. Andersson J, et al. Cutting edge: the prevalence of regulatory T cells in lymphoid tissue is correlated with viral load in HIV-infected patients. The Journal of Immunology. 2005; 174:3143–3147. [PubMed: 15749840]

27. Estes JD, et al. Premature induction of an immunosuppressive regulatory T cell response during acute simian immunodeficiency virus infection. Journal of Infectious Diseases. 2006; 193:703–712. [PubMed: 16453267]
28. Nilsson J, et al. HIV-1–driven regulatory T-cell accumulation in lymphoid tissues is associated with disease progression in HIV/AIDS. Blood. 2006; 108:3808–3817. [PubMed: 16902147]
29. Xing S, et al. Increased Turnover of FoxP3high Regulatory T Cells Is Associated With Hyperactivation and Disease Progression of Chronic HIV-1 Infection. JAIDS Journal of Acquired Immune Deficiency Syndromes. 2010; 54:455–462. doi:10.1097/QAI.0b013e3181e453b9. [PubMed: 20585263]
30. Angin M, et al. HIV-1 infection impairs regulatory T-cell suppressive capacity on a per-cell basis. Journal of Infectious Diseases. 2014:jiu188.
31. Ji J, Cloyd MW. HIV-1 binding to CD4 on CD4+ CD25+ regulatory T cells enhances their suppressive function and induces them to home to, and accumulate in, peripheral and mucosal lymphoid tissues: an additional mechanism of immunosuppression. International immunology. 2009:dxn146.
32. Imamichi H, Lane HC. Regulatory T cells in HIV-1 infection: the good, the bad, and the ugly. Journal of Infectious Diseases. 2012; 205:1479–1482. [PubMed: 22457283]
33. Meditz AL, et al. HLA-DR+ CD38+ CD4+ T Lymphocytes Have Elevated CCR5 Expression and Produce the Majority of R5-Tropic HIV-1 RNA In Vivo. Journal of Virology. 2011; 85:10189–10200. doi:10.1128/jvi.02529-10. [PubMed: 21813616]
34. Shen L-S, et al. CD4 (+) CD25 (+) CD127 (low/−) regulatory T cells express Foxp3 and suppress effector T cell proliferation and contribute to gastric cancers progression. Clinical immunology (Orlando, Fla.). 2009; 131:109–118.
35. Seddiki N, et al. Expression of interleukin (IL)-2 and IL-7 receptors discriminates between human regulatory and activated T cells. The Journal of experimental medicine. 2006; 203:1693–1700. [PubMed: 16818676]
36. Hartigan-O'Connor DJ, Poon C, Sinclair E, McCune JM. Human CD4+ regulatory T cells express lower levels of the IL-7 receptor alpha chain (CD127), allowing consistent identification and sorting of live cells. Journal of immunological methods. 2007; 319:41–52. [PubMed: 17173927]
37. Chen W, et al. Conversion of peripheral CD4+ CD25− naive T cells to CD4+ CD25+ regulatory T cells by TGF-β induction of transcription factor Foxp3. The Journal of experimental medicine. 2003; 198:1875–1886. [PubMed: 14676299]
38. Lanzavecchia A, Sallusto F. Regulation of T cell immunity by dendritic cells. Cell. 2001; 106:263–266. [PubMed: 11509174]
39. Dillon SM, et al. Plasmacytoid and myeloid dendritic cells with a partial activation phenotype accumulate in lymphoid tissue during asymptomatic, chronic Human Immunodeficiency Virus Type 1 infection. Journal of acquired immune deficiency syndromes (1999). 2008; 48:1. [PubMed: 18300699]
40. Boasso A, et al. HIV inhibits CD4+ T-cell proliferation by inducing indoleamine 2, 3-dioxygenase in plasmacytoid dendritic cells. Blood. 2007; 109:3351–3359. [PubMed: 17158233]
41. Presicce P, Shaw JM, Miller CJ, Shacklett BL, Chougnet CA. Myeloid dendritic cells isolated from tissues of SIV-infected Rhesus macaques promote the induction of regulatory T-cells. AIDS (London, England). 2012; 26:263.
42. Boasso A, et al. Regulatory T-cell markers, indoleamine 2, 3-dioxygenase, and virus levels in spleen and gut during progressive simian immunodeficiency virus infection. Journal of virology. 2007; 81:11593–11603. [PubMed: 17715231]
43. Vignali DA, Collison LW, Workman CJ. How regulatory T cells work. Nature Reviews Immunology. 2008; 8:523–532.
44. Ng TS, et al. Regulation of adaptive immunity; the role of interleukin-10. Frontiers in immunology. 2013; 4
45. Kinter A, et al. Suppression of HIV-specific T cell activity by lymph node CD25+ regulatory T cells from HIV-infected individuals. Proceedings of the National Academy of Sciences. 2007; 104:3390–3395.

46. Doitsh G, et al. Abortive HIV infection mediates CD4 T cell depletion and inflammation in human lymphoid tissue. Cell. 2010; 143:789–801. [PubMed: 21111238]
47. Beignon A-S, et al. Endocytosis of HIV-1 activates plasmacytoid dendritic cells via Toll-like receptor–viral RNA interactions. Journal of Clinical Investigation. 2005; 115:3265. [PubMed: 16224540]
48. Caron G, et al. Direct stimulation of human T cells via TLR5 and TLR7/8: flagellin and R-848 up-regulate proliferation and IFN-γ production by memory CD4+ T cells. The Journal of Immunology. 2005; 175:1551–1557. [PubMed: 16034093]
49. Fellay J, et al. Response to antiretroviral treatment in HIV-1-infected individuals with allelic variants of the multidrug resistance transporter 1: a pharmacogenetics study. The Lancet. 2002; 359:30–36.
50. Pozo-Balado MM, et al. Maraviroc Reduces the Regulatory T-Cell Frequency in Antiretroviral-Naive HIV-Infected Subjects. Journal of Infectious Diseases. 2014:jiu180.
51. Manches O, et al. HIV-activated human plasmacytoid DCs induce Tregs through an indoleamine 2, 3-dioxygenase–dependent mechanism. The Journal of clinical investigation. 2008; 118:3431–3439. [PubMed: 18776940]
52. Granelli-Piperno A, Golebiowska A, Trumpfheller C, Siegal FP, Steinman RM. HIV-1-infected monocyte-derived dendritic cells do not undergo maturation but can elicit IL-10 production and T cell regulation. Proceedings of the National Academy of Sciences of the United States of America. 2004; 101:7669–7674. [PubMed: 15128934]
53. Favre D, et al. Tryptophan catabolism by indoleamine 2, 3-dioxygenase 1 alters the balance of TH17 to regulatory T cells in HIV disease. Science Translational Medicine. 2010; 2:32ra36–32ra36.
54. Krathwohl MD, Schacker TW, Anderson JL. Abnormal presence of semimature dendritic cells that induce regulatory T cells in HIV-infected subjects. Journal of Infectious Diseases. 2006; 193:494–504. [PubMed: 16425128]
55. Audige A, et al. Anti-HIV state but not apoptosis depends on IFN signature in CD4+ T cells. The Journal of Immunology. 2006; 177:6227–6237. [PubMed: 17056552]
56. Gougeon M-L, et al. Programmed cell death in peripheral lymphocytes from HIV-infected persons: increased susceptibility to apoptosis of CD4 and CD8 T cells correlates with lymphocyte activation and with disease progression. The Journal of Immunology. 1996; 156:3509–3520. [PubMed: 8617980]
57. Haas MK, Levy DN, Folkvord JM, Connick E. Distinct Patterns of Bcl-2 Expression Occur in R5- and X4-Tropic HIV-1-Producing Lymphoid Tissue Cells Infected Ex Vivo. AIDS research and human retroviruses. 2014
58. Schmitt N, et al. The cytokine TGF-[beta] co-opts signaling via STAT3-STAT4 to promote the differentiation of human TFH cells. Nature immunology. 2014
59. Shibata R, et al. Neutralizing antibody directed against the HIV–1 envelope glycoprotein can completely block HIV–1/SIV chimeric virus infections of macaque monkeys. Nature medicine. 1999; 5:204–210.
60. Wei X, et al. Antibody neutralization and escape by HIV-1. Nature. 2003; 422:307–312. [PubMed: 12646921]
61. Richman DD, Wrin T, Little SJ, Petropoulos CJ. Rapid evolution of the neutralizing antibody response to HIV type 1 infection. Proceedings of the National Academy of Sciences. 2003; 100:4144–4149.
62. Haynes BF, Montefiori DC. Aiming to induce broadly reactive neutralizing antibody responses with HIV-1 vaccine candidates. 2006
63. Binley JM, et al. Comprehensive Cross-Clade Neutralization Analysis of a Panel of Anti-Human Immunodeficiency Virus Type 1 Monoclonal Antibodies. Journal of Virology. 2004; 78:13232–13252. doi:10.1128/jvi.78.23.13232-13252.2004. [PubMed: 15542675]
64. Locci M, et al. Human circulating PD-1+ CXCR3− CXCR5+ memory Tfh cells are highly functional and correlate with broadly neutralizing HIV antibody responses. Immunity. 2013; 39:758–769. [PubMed: 24035365]

65. Hong JJ, Amancha PK, Rogers K, Ansari AA, Villinger F. Spatial alterations between CD4+ T follicular helper, B, and CD8+ T cells during simian immunodeficiency virus infection: T/B cell homeostasis, activation, and potential mechanism for viral escape. The Journal of Immunology. 2012; 188:3247–3256. [PubMed: 22387550]

66. León B, Bradley JE, Lund FE, Randall TD, Ballesteros-Tato A. FoxP3+ regulatory T cells promote influenza-specific Tfh responses by controlling IL-2 availability. Nature communications. 2014; 5

67. Wing JB, Ise W, Kurosaki T, Sakaguchi S. Regulatory T Cells Control Antigen-Specific Expansion of Tfh Cell Number and Humoral Immune Responses via the Coreceptor CTLA-4. Immunity. 2014; 41:1013–1025. [PubMed: 25526312]

68. Levy DN, Aldrovandi GM, Kutsch O, Shaw GM. Dynamics of HIV-1 recombination in its natural target cells. Proceedings of the National Academy of Sciences. 2004; 101:4204–4209.

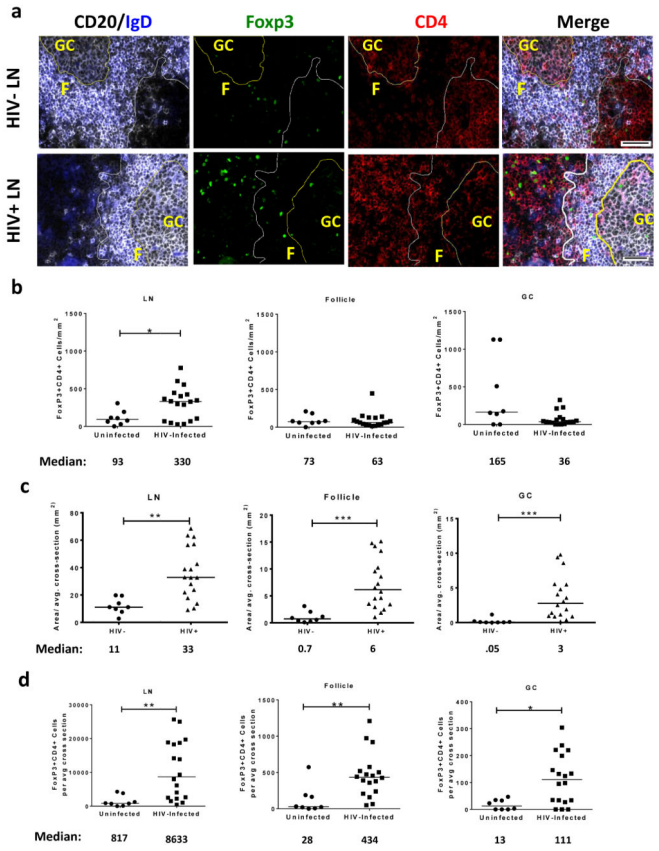

Figure 1. T_{FR} expansion in human lymph nodes during HIV infection

(a) Representative images of immunofluorescently stained lymph node sections from a subject with chronic, untreated HIV infection (n=17) and an uninfected control subject (n=8). Lymph nodes (LN) were stained with fluorescently labeled antibodies to CD20 (white), IgD (blue), Foxp3 (green), and CD4 (red). Follicle (F) was defined as CD20+ (white line) and germinal-center (GC) was defined as CD20+IgD− (yellow line). Images were scanned at 60X magnification and scale bars equal 20 μm. (b) Foxp3+CD4+ cells were quantified in different regions of immunofluorescently stained lymph node shown in Fig. 1a from uninfected (n=8) and HIV-infected (n=17) subjects using visual inspection and quantitative image analysis to determine areas. (c) The average areas of total (LN), follicular, and GC regions per lymph node cross-section were determined by quantitative image analysis. (d) The average number of CD4+Foxp3+ cells per LN, follicle, and GC cross-section was calculated by multiplying the frequency of CD4+Foxp3+ cells/mm^2 (Fig. 1b) by the average area of each region (Fig. 1c) for each subject. The horizontal bars of each graph indicate the median value and are listed where appropriate for clarity. Statistical analyses were performed by Mann-Whitney (Wilcoxon) tests to compare unpaired, nonparametric values and significance is denoted by asterisks where * = $p < 0.05$ and ** = $p < 0.01$.

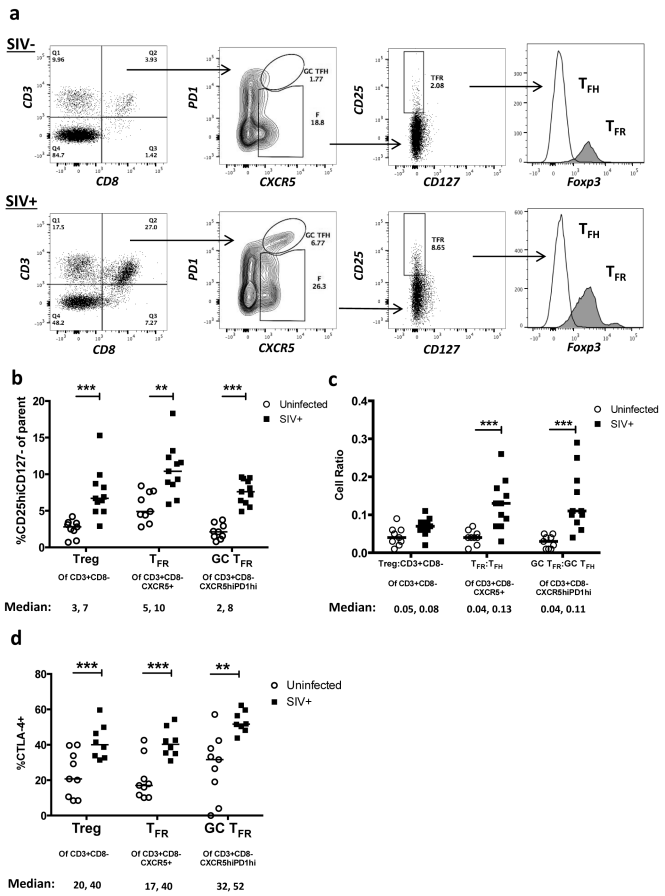

Figure 2. T_{FR} expansion in lymphoid tissues during chronic SIV infection

(a) Disaggregated lymph node and spleen cells from SIV-uninfected (n=9) or chronically SIV-infected rhesus macaques (n=11) were analyzed by flow cytometry. Representative examples of flow cytometry gating are shown. Of viable CD3+CD8− cells, follicular subsets were defined as CXCR5+ cells (F) and germinal center subsets were defined as $CXCR5^{hi}PD\text{-}1^{hi}$ cells (GC). Of these subsets, regulatory cells were defined as $CD25^{hi}CD127-$. T_{FR} ($CXCR5+CD25^{hi}CD127-$) were Foxp3+ while T_{FH} ($CXCR5+CD25^{lo/-}$) were Foxp3−. (b) The percentages of each rhesus macaque regulatory subset, as analyzed in (a) are shown (n=10). (c) The ratios of each regulatory cell population to its non-regulatory cell counterpart are shown. (d) The percentage of total CTLA-4 expression is shown in SIV-uninfected (n=9) and chronically SIV-infected (n=8) rhesus macaques. The horizontal bars of each graph indicate the median value and are listed where appropriate for clarity. Statistical analyses were performed by Mann-Whitney (Wilcoxon) tests to compare unpaired, nonparametric values and significance is denoted by asterisks where * = $p < 0.05$, ** = $p < 0.01$, and *** = $p < 0.001$.

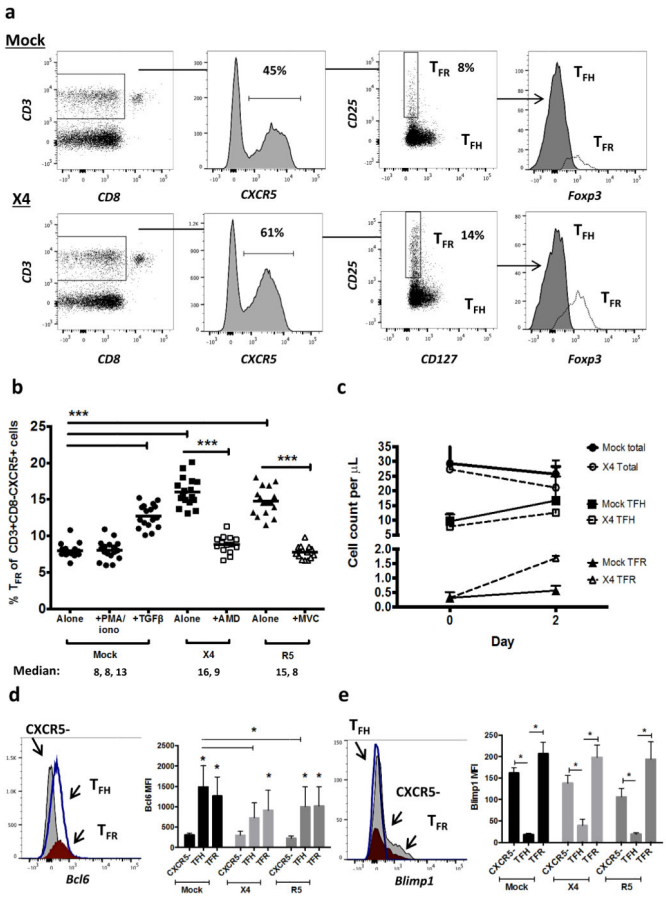

Figure 3. HIV entry and replication promote T_{FR} expansion

Disaggregated tonsil cells were spinoculated with X4 or R5 HIV and T_{FR} populations were analyzed by flow cytometry (n=15). (a) A representative example of tonsil cell flow gating. From viable CD3+CD8− cells, T_{FR} are defined as CXCR5+ and $CD25^{hi}CD127-$. T_{FR} cells contain Foxp3+ cells while remaining T_{FH} ($CXCR5+CD25^{lo/-}$) cells are Foxp3−. (b) Percentages of T_{FR} determined by gating strategies in (a) are shown. Experimental conditions include mock-spinoculated cells cultured with PMA (50 ng/mL) and ionomycin (1 μg/mL) or exogenous TGFβ (100ng/mL) for 24 hours and cells pretreated to block CXCR4 (AMD, 200 μM) and CCR5 (MVC, 2 μM). (c) Using flow cytometry counting beads, the number of cells per μL were determined for total (CD3+CD8−), T_{FH} ($CXCR5+CD25^{lo/-}$), and T_{FR} ($CXCR5+CD25^{hi}CD127-$) subsets in mock- and X4-spinoculated samples (n=3). (d) Bcl-6 expression is shown in CXCR5− (gray), T_{FH} (blue), and T_{FR} (red) populations after mock-, X4-, or R5-spinoculation (n=5). (e) Blimp-1 expression was also determined as in (d). The horizontal bars of each graph indicate the median value and are listed where appropriate for clarity. Statistical analyses were performed by Friedman nonparametric tests (b, d, e) and significance is denoted by asterisks where * = $p < 0.05$, ** = $p < 0.01$ and *** = $p < 0.001$.

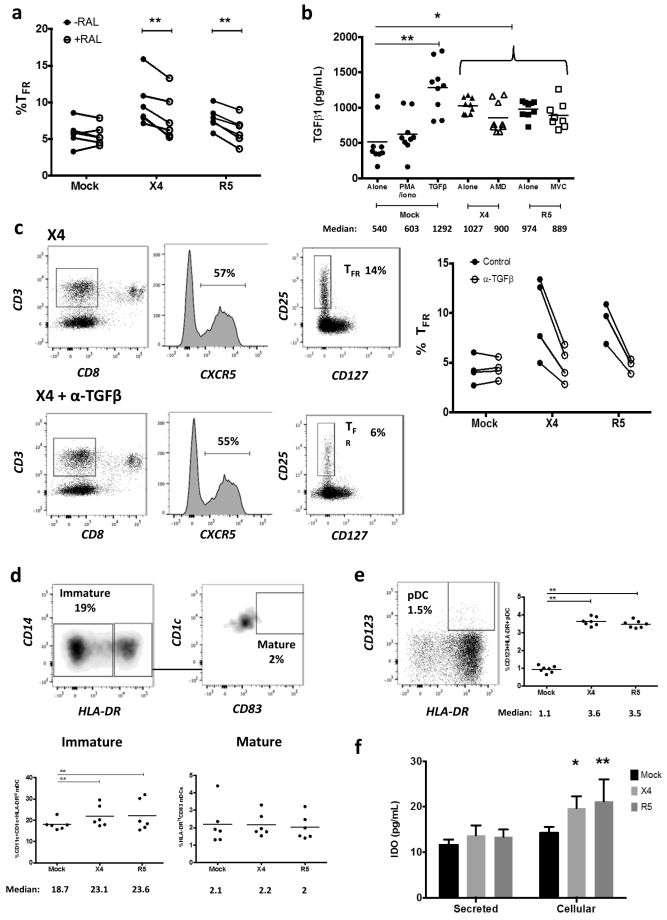

Figure 4. Viral replication, TGFβ signaling, and regulatory dendritic cells promote T_{FR} expansion

Tonsil cells were mock-spinoculated or spinoculated with X4 or R5 virus and cultured for 2 days under a variety of conditions. (a) Tonsil cells were treated with the integrase inhibitor raltegravir (RAL, 10 μM) during culture to allow viral entry but prevent replication and percentages of T_{FR} determined (n=5). (b) Tonsil cells were cultured under the conditions shown and TGFβ-1 levels were measured in culture supernatant by ELISA (n=8). (c) Tonsil cells were cultured in the presence of TGFβ blocking antibodies (2 μg/mL) and the percentages of T_{FR} were measured (n=4). Addition of anti- TGFβ antibodies did not influence cell viability. (d) Tonsil cells were cultured under the conditions shown and then analyzed for the presence of immature myeloid DCs (CD11c+CD1c+HLA-DRlo) and mature myeloid DCs (CD11c+CD1c+HLA-DR+CD83+) (n=6). (e) Samples in (d) were also analyzed for activated plasmacytoid DCs (CD123+HLA-DR+, n=6). (f) Cell culture supernatants and lysates from (d, e) were analyzed by ELISA to quantitate IDO production (n=6). The horizontal bars of each graph indicate the median value and are listed where appropriate for clarity. Statistical analyses were performed Wilcoxon matched-pairs tests (a, c) or Whitney ranked sums tests (b, d-f) and significance is denoted by asterisks where * = $p < 0.05$, ** = $p < 0.01$ and *** = $p < 0.001$.

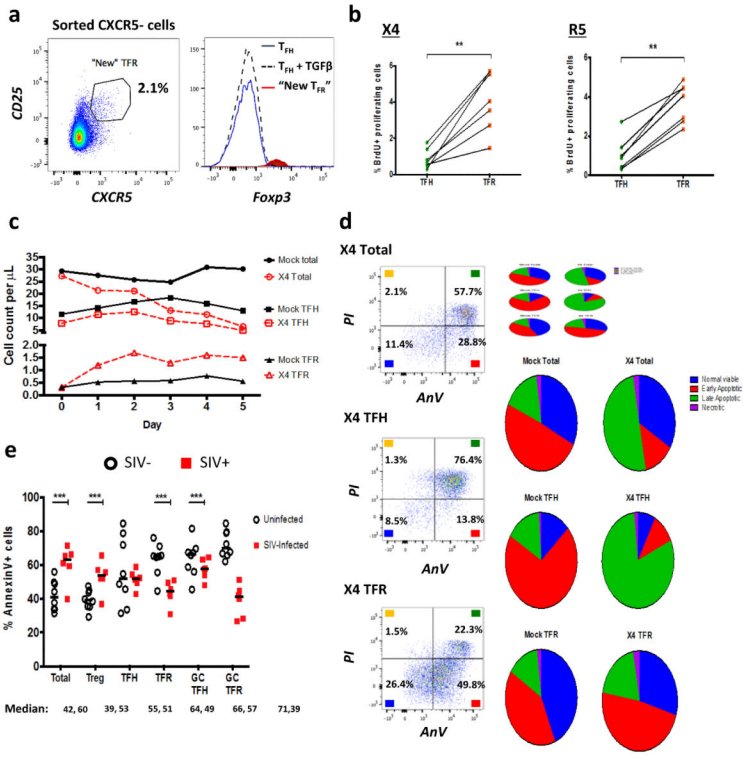

Figure 5. Acquisition of CXCR5, enhanced proliferation, and reduced apoptosis promote T_{FR} expansion

(a) T_{FH} and CXCR5− T cell populations were sorted and cultured without stimulation, or T_{FH} were cultured in the presence of exogenous TGFβ (100 ng/mL). CXCR5 expression was analyzed on sorted CXCR5− cells after 2 days and cells expressing CXCR5 are labeled as “new T_{FR}”. The Foxp3 expression levels of T_{FH}, T_{FH} cultured with TGFβ, and “new” T_{FR} were determined (n=3). (b) T_{FH} and T_{FR} were mock-, X4-, or R5-spinoculated and cell proliferation measured by BrdU incorporation after 2 days of culture (n=7). (c, d) A 5 day time course was performed to monitor T cell population counts and rates of cell death with mock- or X4-spinoculated tonsil cells (n=3). (c) Average counts of total (CD3+CD8−, circles), T_{FH} (CXCR5+CD25$^{lo/-}$, squares), and T_{FR} (CXCR5+CD25^{hi}CD127−, triangles) are shown for the duration of culture (n=3). (d) Stages of cell death are shown at day 5 and defined as early apoptosis (AnnexinV+), late or advanced apoptosis (AnnexinV+ PI+), and necrotic death (PI+) (n=3). (e) Cell subsets from disaggregated lymphoid tissues of chronically SIV-infected (n=6) and uninfected rhesus macaques (n=8) were analyzed for apoptosis by percent Annexin-V binding. Cell phenotypes were defined as total (CD3+CD8−), Treg (CD3+CD8−CD25^{hi}CD127−), T_{FH} (CD3+CD8−CXCR5+CD25$^{lo/-}$), T_{FR} (CD3+CD8−CXCR5+CD25^{hi}CD127−), GC T_{FH} (CD3+CD8−CXCR5+PD1^{hi}CD25$^{lo/-}$), and GC T_{FR} (CD3+CD8−CXCR5+PD1^{hi}CD25^{hi}CD127−). Statistical analyses were performed by Wilcoxon matched-pairs tests (b) or Mann Whitney tests (e) and significance is denoted by asterisks where ** = $p < 0.01$ and *** = $p < 0.001$.

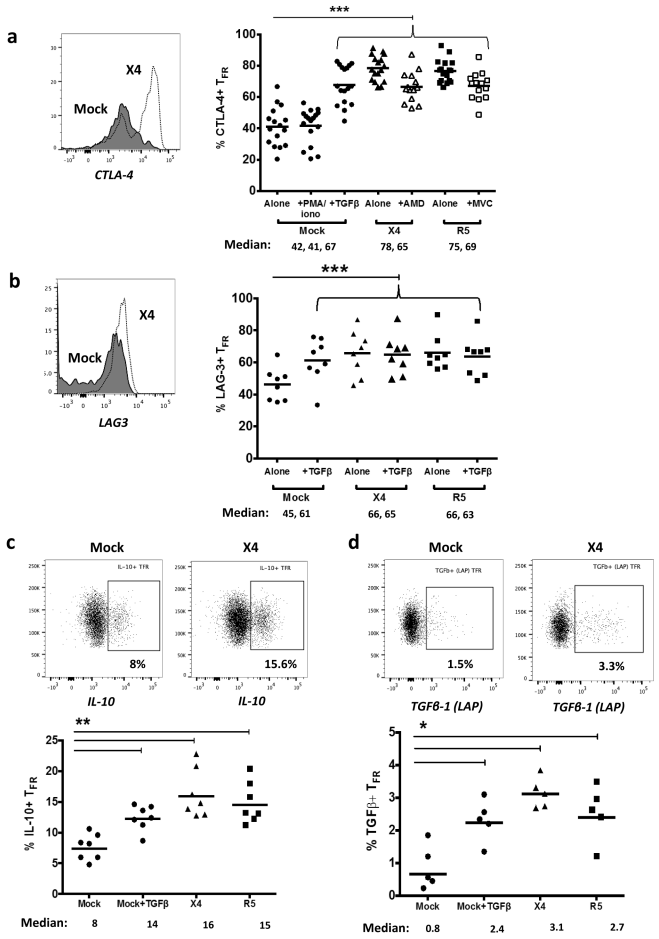

Figure 6. T_{FR} exhibit an enhanced regulatory phenotype in *ex vivo* HIV infection

Tonsil cells were mock-, X4-, or R5-spinoculated and cultured under experimental conditions as indicated. T_{FR} were then analyzed for expression of regulatory receptors and cytokine production by intracellular cytokine staining. (a) Percentage of total (surface and intracellular) T_{FR} CTLA-4 expression (n=15). (b) Percentage of surface T_{FR} LAG-3 expression (n=8). (c) Production of IL-10 by T_{FR} (n=7). (d) Production of TGFβ-1 (measured as LAP) by T_{FR} (n=5). The horizontal bars of each graph indicate the median value and are listed where appropriate for clarity. Statistical analyses were performed by Friedman (a, b) or Mann-Whitney tests (c, d) and significance is denoted by asterisks where * = $p < 0.05$, ** = $p < 0.01$ and *** = $p < 0.001$.

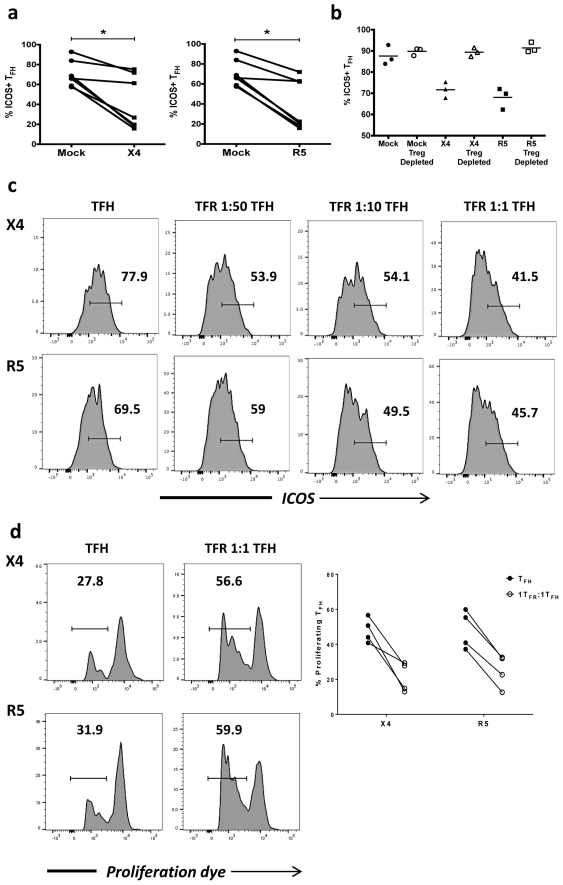

Figure 7. T_{FR} disrupt T_{FH} maintenance and proliferation

(a) Tonsil T_{FH} were analyzed for surface ICOS, following mock-, X4-, or R5-spinoculation (n=7). (b) CD25+ regulatory cells were depleted from each culture condition and ICOS expression on T_{FH} was analyzed (n=3). (c) Tonsil T_{FH} and T_{FR} were isolated, spinoculated, and co-cultured for 2 days at the indicated ratios. Representative images of ICOS expression on T_{FH} surface are shown (n=2). (d) Tonsil T_{FH} were isolated, labeled with eFluor 670 proliferation dye, and cultured alone or with an equal number of T_{FR}. Proliferation was measured by dye dilution (n=4). The horizontal bars of each graph indicate the median value and are listed where appropriate for clarity. Statistical analyses were performed Friedman nonparametric tests (a) and significance is denoted by asterisks where * = $p < 0.05$.

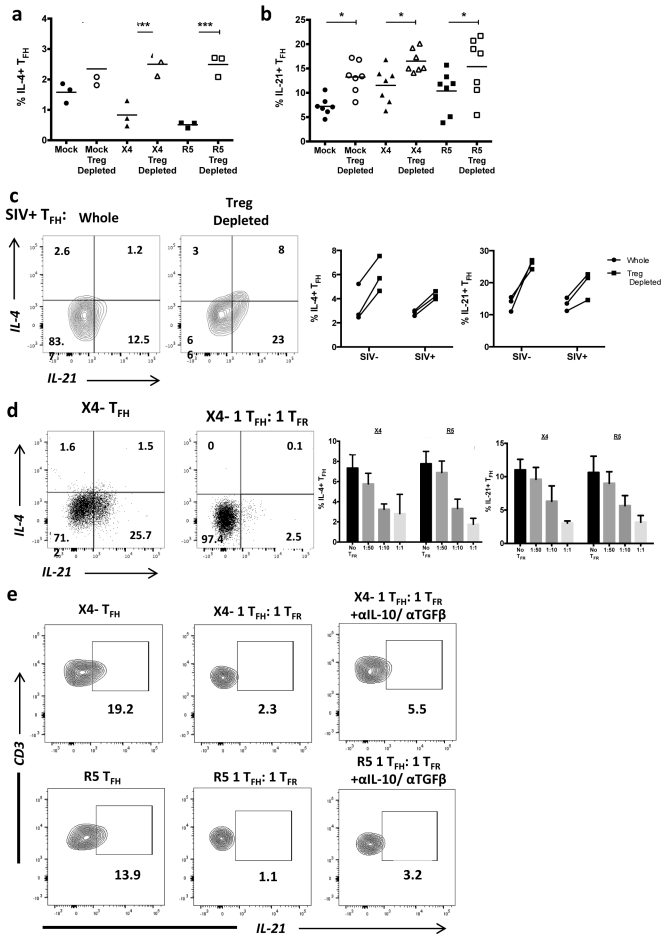

Figure 8. T_{FR} impair T_{FH} cytokine production

(a) Tonsil T_{FH} were analyzed by intracellular cytokine staining for IL-4 and IL-21 production following mock-, X4-, or R5-spinoculation. (b) CD25+ regulatory cells were depleted prior to spinoculation and IL-4 (n=3) and IL-21 (n=7) production by T_{FH} cells were analyzed after 2 days. (c) IL-4 and IL-21 production by T_{FH} were analyzed in disaggregated lymph node cells from rhesus macaques with and without CD25-depletion (n=3). (d) Sorted populations of tonsil T_{FH} and T_{FR} were spinoculated, T_{FR} were added back to T_{FH} at an increasing ratio, and T_{FH} production of IL-4 and IL-21 were measured by intracellular cytokine assays at day 2 (n=4). (e) Sorted tonsil T_{FH} and T_{FR} were cultured for 2 days in the presence of IL-10 and TGFβ neutralizing antibodies and T_{FH} production of IL-21 was analyzed (n=2). Statistical analyses were performed by Friedman nonparametric tests (a, b) and significance is denoted by asterisks where * = $p < 0.05$ and *** = $p < 0.001$.